Electron-hole correlations and optical excitonic gaps in quantum-dot quantum wells: Tight-binding approach

Rui-Hua Xie and Garnett W. Bryant*
National Institute of Standards and Technology, Gaithersburg, Maryland 20899-8423

Seungwon Lee
National Center for Supercomputing Applications, University of Illinois at Urbana-Champaign, Urbana, Illinois 61801-2300
and Department of Physics, Ohio State University, Columbus, Ohio 43210-1106

W. Jaskólski
Instytut Fizyki, UMK, Grudziądzka 5, 87-100 Torún, Poland

(Received 21 December 2001; revised manuscript received 15 March 2002; published 28 May 2002)

Electron-hole correlation in quantum-dot quantum wells (QDQW's) is investigated by incorporating Coulomb and exchange interactions into an empirical tight-binding model. Sufficient electron and hole single-particle states close to the band edge are included in the configuration to achieve convergence of the first spin-singlet and triplet excitonic energies within a few meV. Coulomb shifts of about 100 meV and exchange splittings of about 1 meV are found for CdS/HgS/CdS QDQW's (4.7 nm CdS core diameter, 0.3 nm HgS well width, and 0.3 nm to 1.5 nm CdS clad thickness) that have been characterized experimentally by Weller and co-workers [D. Schooss, A. Mews, A. Eychmüller, H. Weller, Phys. Rev. B, 49, 17 072 (1994)]. The optical excitonic gaps calculated for those QDQW's are in good agreement with the experiment.

DOI: 10.1103/PhysRevB.65.235306 PACS number(s): 73.22.−f, 71.15.Ap, 71.35.Cc, 73.63.−b

Semiconductor nanostructures, from quantum wells, quantum wires to quantum dots,[1,2] have been extensively investigated due to their remarkable applications, for example, as fast and low noise electronic devices and tunable optoelectronic elements. Recently, a class of new and promising hetero-quantum dots, termed *quantum-dot quantum wells* (QDQW's), have been successfully synthesized in water, for example, CdS/HgS/CdS,[3–5] CdTe/HgTe/CdTe,[6] and ZnS/CdS/ZnS.[7] These QDQW's have internal nanoheterostructures with a quantum-well region contained inside the quantum dot. Meanwhile, high-resolution transmission electron microscopy images[5,6] have shown that CdS/HgS/CdS and CdTe/HgTe/CdTe QDQW's are not spherical, but are preferentially truncated tetrahedral particles. However, spherical shell particles are commonly considered to explain experimental results.[3,4,8–12]

Numerical calculations[3,4,8,9] on QDQW's have been based generally on the one-band effective-mass approximation as well as the parabolic approximation for the conduction and valence bands. These theoretical studies have demonstrated the remarkable effect of the internal well on single-particle electron and hole energies and pair overlaps[3,4,8] and determined the ground-state energy of an uncorrelated electron-hole pair.[3,4] Moreover, Bryant[9] determined the contribution of pair correlation to the electronic structure of QDQW nanosystems. Very recently, Jaskólski and Bryant[10] have developed a multiband theory to determine electron, hole, and exciton states for QDQW's. Actually, an atomic model is essential for QDQW's since the internal wells are no more than a few monolayers thick.[11,12] Hence, in this paper, we incorporate for the first time Coulomb and exchange interactions into an empirical tight-binding model to describe QDQW nanocrystals. In detail, we shall investigate electron-hole interactions and optical excitonic gaps of QDQW's, and report our numerical results by considering three CdS/HgS/CdS QDQW's that were characterized experimentally by Weller and co-workers.[3] Comparison with the experiment shows that our tight-binding theory provides a good description for QDQW nanocrystals.

First, we use the empirical tight-binding (ETB) method[13–16] to perform numerical calculations of both electron and hole single-particle energies (i.e, E_e and E_h) and eigenstates (i.e., $|\Phi_e\rangle$ and $|\Phi_h\rangle$) for QDQW's. Our theory can be used to model single or coupled nanocrystal systems with spherical, hemispherical, tetrahedral or pyramidal geometry. In this paper, we focus on single spherical QDQW's. Also, we assume that atoms in these nanoparticles occupy the sites of a regular fcc lattice. As developed by Vogl, Hjalmarson, and Dow,[17] each atom has its outer valence s orbital and three outer p orbitals plus a fictitious excited s^* orbital that is included to mimic the effects of higher lying states. Only onsite and nearest-neighbor couplings between orbitals are included in our sp^3s^* ETB theory. Since the spin-orbital coupling is not known for HgS, we shall not consider it for our numerical results reported here. The empirical single-particle Hamiltonians are determined by adjusting the matrix elements to reproduce known band gaps and effective masses of the bulk band structures. In this paper, our tight-binding parameters for CdS and HgS are the same as those of Bryant and Jaskólski.[11,12] Finally, the electron and hole single-particle eigenstates and energies close to the band edges are found by diagonalizing the single-particle Hamiltonian with an iterative eigenvalue solver.

We describe the effective Hamiltonian of an electron-hole pair by combining a two-particle term H_{eh}, which includes the Coulomb and exchange interactions, with a single-particle term H_{single} that contains the kinetic and potential energies of the electron and hole.[16] The Coulomb and exchange interactions are screened by a dielectric function $\epsilon(|\mathbf{r}'-\mathbf{r}|,R)$, where $|\mathbf{r}'-\mathbf{r}|$ and R are the separation be-

TABLE I. Onsite unscreened Coulomb and exchange integrals, ω_{coul} and ω_{exch} for the sp^3s^* basis set in units of eV for Cd, Hg, and S. Integrals for the sp^3 orbitals are calculated based on the hybridized orbitals along the bonding directions defined by Leung and Whaley (Ref. 14).

Integral	(sp_a^3, sp_a^3)	(sp_a^3, sp_b^3)	(sp_a^3, s^*)	(s^*, s^*)
ω_{coul}^{Cd}	5.3346	4.0787	1.7942	1.7181
ω_{exch}^{Cd}	5.3346	0.5905	0.1379	1.7181
ω_{coul}^{S}	15.5190	11.7173	3.5295	2.8804
ω_{exch}^{S}	15.5190	1.1836	0.0454	2.8804
ω_{coul}^{Hg}	6.1733	4.4216	1.9593	1.1089
ω_{exch}^{Hg}	6.1732	0.6295	0.0088	1.1089

tween electron and hole and the quantum dot radius, respectively. Our electron-hole basis set $\{|\Psi_i\rangle\}$ is taken by multiplying the spatial part $|\Phi_{eh}\rangle$ (namely, the product of electron and hole single-particle eigenstates $|\Phi_e\rangle$ and $|\Phi_h\rangle$) and their spin states $|\phi_{spin}\rangle$ (namely, either the singlet component or one of the triplet components of the electron-hole spin state). Then, the single-particle Hamiltonian can be written in terms of the electron-hole basis set as

$$H_{single} = \sum_i E_i |\Psi_i\rangle\langle\Psi_i|, \tag{1}$$

where $E_i = E_e^{(i)} - E_h^{(i)}$ is the energy difference between corresponding electron and hole energies, $E_e^{(i)}$ and $E_h^{(i)}$ of the single-particle Hamiltonian, of the ith electron-hole pair. Meanwhile, the electron-hole interaction Hamiltonian in the electron-hole basis set is given by

$$H_{eh} = \sum_{spin} (J+K) |\phi_{spin}\rangle\langle\phi_{spin}|, \tag{2}$$

where J and K describe the Coulomb and exchange interactions (the same as those of Lee *et al.*[16]). More details about the formulas mentioned in this part are given in the work of Lee *et al.*[16]

As introduced by Leung and Whaley[14] and Lee *et al.*,[16] the Coulomb and exchange interaction matrix elements are expressed in terms of the Coulomb and exchange integrals, ω_{coul} and ω_{exch}, of our ETB orbitals. Table I lists the unscreened onsite Coulomb and exchange integrals for the sp^3s^* basis set for Cd, S, and Hg calculated by using a Monte Carlo method with importance sampling for the radial integrations.[16] Regarding offsite Coulomb integrals, we estimate them using the Ohno formula modified by Leung and Whaley.[14] It is known that offsite exchange integrals decrease quickly as the distance between atom sites increases due to the localization and orthogonality of orbitals.[16] Here, we use the offsite exchange integrals of Leung, Pokrant, and Whaley.[15]

The high-frequency dielectric constant[3] for the different regions of CdS/HgS/CdS QDQW's are $\epsilon_{CdS} = 5.5$, $\epsilon_{HgS} = 11.36$, and $\epsilon_{H_2O} = 1.78$. In our numerical calculations, we use an average, effective high-frequency dielectric constant, $\epsilon_{ave} = 6$.

Because of the total spin of the electron-hole pair, we have two Hamiltonians: one for a spin singlet including both the Coulomb and exchange interactions, and another for a spin triplet having only the Coulomb interaction. Therefore, we diagonalize both Hamiltonians in the electron-hole basis separately and obtain a set of spin-singlet and triplet excitonic states. For clarity, we use the parameter set (D_{core}, L_{well}, L_{clad}) to denote a CdS/HgS/CdS QDQW, where D_{core}, L_{well}, and L_{clad} are the CdS core diameter, HgS well width and CdS clad thickness, respectively, in nanometer. Also, we mention three definitions of Lee *et al.*:[16] (i) *optical excitonic gap* E_g^{opt} is the lowest spin-singlet excitonic energy $E_1^{(1)}$; (ii) the difference between the single-particle energy gap E_g^{single} and the lowest spin-triplet excitonic energy $E_1^{(3)}$ is defined as the *Coulomb shift*, namely, $E_{coul} = E_g^{single} - E_1^{(3)}$; (iii) the difference between the lowest spin-singlet and triplet excitonic energies is defined as the *exchange splitting*, namely, $E_{exch} = E_1^{(1)} - E_1^{(3)}$.

For the band gaps of HgS and CdS, we use $E_{g,\mathrm{HgS}} = 0.2$ eV and $E_{g,\mathrm{CdS}} = 2.5$ eV, respectively, with the CdS conduction band edge 1.45 eV above the conduction-band edge of HgS.[10] Figure 1 shows the electron and hole single-particle energy spectra of (4.7, 0.3, 0.3), (4.7, 0.3, 1), and (4.7, 0.3, 1.5) CdS/HgS/CdS QDQW's, which have been characterized experimentally by Weller and co-workers.[3] The calculated single-particle energy gaps are 2.173 eV, 2.099 eV, and 2.085 eV, respectively. The degeneracy is also shown in the brackets. The lowest electron and hole states can be described approximately by the spherical symmetries indicated in Fig. 1, i.e., $1S$-, $1P$-, and $1D$-like electron states, mixed $(1P_0 + 1P_2)$-like hole states, and a $1S_1$-like hole state. Here, S, P, D indicate the spatial angular momentum and the subscript for holes indicates the total angular-momentum sum of the spatial and atomic orbital angular momenta. As the clad thickness increases, the level ordering of the electron states does not change, but that of the last two hole states switches (as shown in Fig. 1). The ordering of hole levels switches because excited P hole levels are the states most sensitive to the potential far from the dot center.

In this work, we focus mainly on the lowest singlet and triplet excitonic energies. In our electron-hole basis set, we include the four electron ($n_e = 0, 1, 2, 3$) and nine hole ($n_h = 0, 1, \ldots, 8$) single-particle states closest to the band edge, where n_e (labeling initially from the ground electron state) and n_h (labeling initially from one of the triply degenerate ground hole states) are the indices for electron and hole single-particle states. For example, Table II lists the Coulomb shift, exchange splitting and the lowest spin-singlet and triplet excitonic energies for the (4.7, 0.3, 0.3) QDQW by considering different numbers of electron and hole single-particle states close to the band edge. The cases shown are chosen so as to ensure that all states of a given degenerate level are included. The inclusion of more electron-hole configurations leads to an increase of the Coulomb shift and exchange splitting. The excitonic energies are converged within a few meV when $N_e = 4$ and $N_h = 9$.

Figure 2 shows the singlet excitonic energy spectrum for the lowest few excitonic states in the three QDQW's. For the

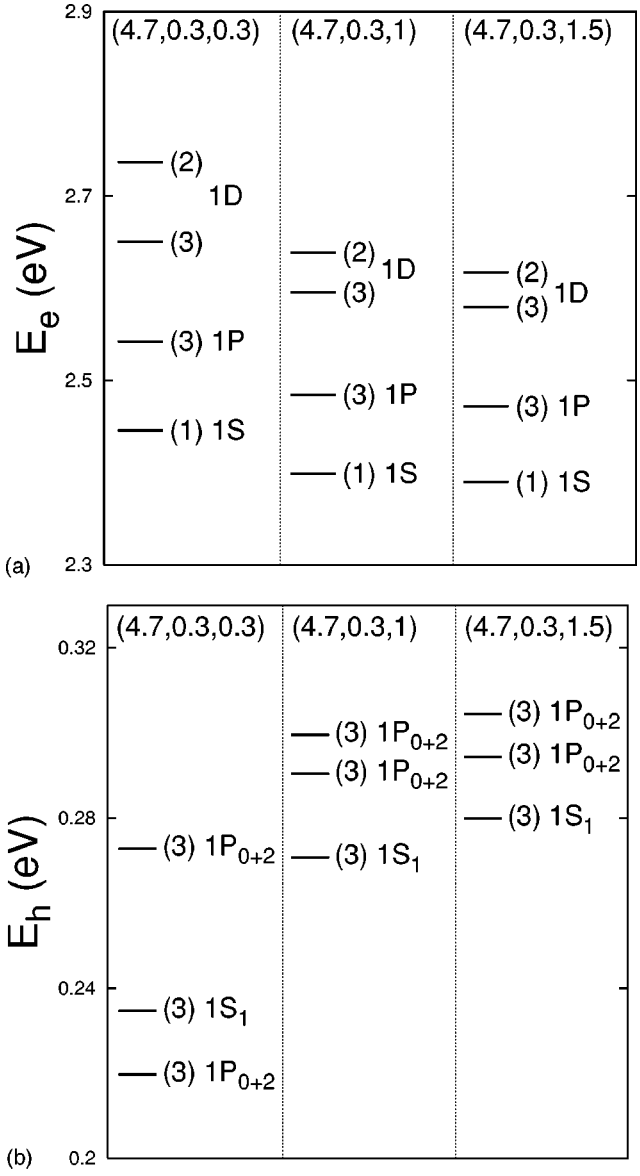

FIG. 1. Electron and hole single-particle energy spectra, E_e and E_h, for (4.7, 0.3, 0.3), (4.7, 0.3, 1) and (4.7, 0.3, 1.5) CdS/HgS/CdS QDQW's. The level degeneracy is shown in the brackets and the approximate spherical symmetry of each state is indicated. Both the electron energy, which increases upward, and the hole energy, which decreases downward, are referred to the top of the valence band of CdS.

electron-hole basis, $N_e=4$ and $N_h=9$, the first three triply degenerate excitonic energy levels come mainly from the contribution of electron-hole pairs formed with the ground-state electron, as indicated in Fig. 2. Other higher excitonic energy levels are due to electron-hole pairs made from the excited-state electron. This is clearly shown in Fig. 3, which presents the occupation probability $P(K)$ of the Kth electron-hole pair (n_e,n_h), $K\equiv(n_e,n_h)=n_h+1+9n_e$, for one exciton state from each of the three lowest triply degenerate exciton levels (the first, fifth, and eighth exciton states in Fig. 2) and a higher exciton level (the 22nd exciton state). Figure 3 shows that correlation does not strongly mix pair states of different energy in forming the low excitonic states.

TABLE II. Coulomb shift E_{coul}, exchange splitting E_{exch} and the first spin-singlet and triplet excitonic energies $E_1^{(1)}$ and $E_1^{(3)}$ for a (4.7, 0.3, 0.3) CdS/HgS/CdS QDQW. N_e and N_h denote the number of electron and hole single-particle states included in the basis set.

N_e	N_h	$E_1^{(1)}$ (meV)	$E_1^{(3)}$ (meV)	E_{coul} (meV)	E_{exch} (meV)
1	3	2079.62	2079.11	94.01	0.51
4	3	2073.23	2072.46	100.66	0.77
4	6	2067.28	2066.22	106.90	1.06
4	9	2067.19	2066.12	107.00	1.07

This explains why convergence is achieved with only a few basis states. Our previous calculations[9] of correlation effects in QDQW's showed that correlation effects are weaker in QDQW's than in quantum dots. The extra local confinement of the electron and hole to the quantum well inside the quantum dot increases the splitting between the lowest single-particle states and suppresses Coulomb mixing of these states.

Table III summarizes our calculated Coulomb shift E_{coul}, exchange splitting E_{exch}, $1S$-$1S$ transition energy $E_{1S\text{-}1S}$, and optical excitonic gap E_g^{opt} for the three CdS/HgS/CdS QDQW's. $E_{1S\text{-}1S}$ is the energy of the lowest optically active transition because it is a transition between the even-parity $1S$ electron state and the odd-parity $1S_1$ hole state. E_g^{opt} is the energy of the lowest possible spin-singlet transition that is between the lowest electron (even parity $1S$) and lowest hole (even parity $1P_0$). E_g^{opt} corresponds to the emission peak in experiment. In the experiment, the points of maxi-

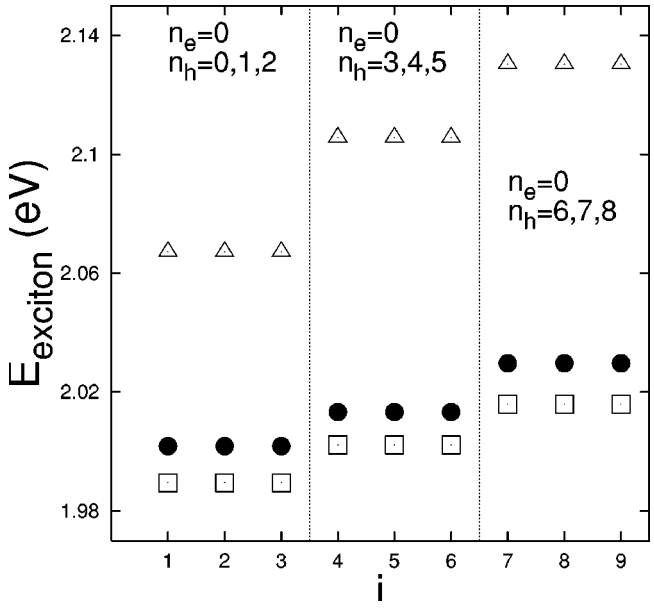

FIG. 2. Spin-singlet excitonic energy spectrum for the first few excitonic states (j, the state serial number), where △, ●, and □ are for (4.7, 0.3, 0.3), (4.7, 0.3, 1), and (4.7, 0.3, 1.5) CdS/HgS/CdS QDQW's, respectively. The primary electron-hole pair states making up each of the triply degenerate excitonic levels are indicated.

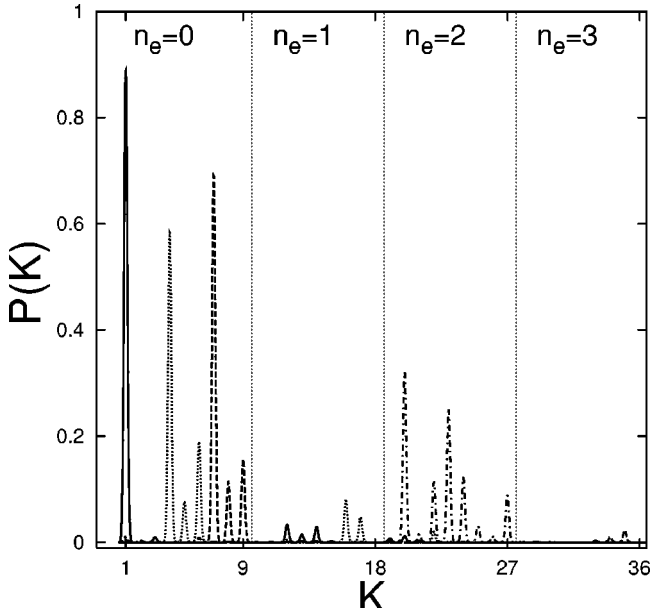

FIG. 3. Occupation probability $P(K)$ of the Kth electron-hole pair (n_e,n_h) in the first (solid line), 5th (dotted line), 8th (dashed line) and 22nd (dot-dashed line) spin-singlet excitonic states for the (4.7, 0.3, 0.3) CdS/HgS/CdS QDQW. $P(K)$ is broadened by a Gaussian to enhance visualization.

mum curvature in the absorption spectra are a good measure for the $1S$-$1S$ transition energies[20] and the experimentally measured gaps[3] E_g^{exp} for the three CdS/HgS/CdS QDQW's are listed in Table III. We find that our calculations for $1S$-$1S$ exciton energies are in good agreement with experimental E_g^{exp} (the relative errors between the experiment and our theory are 0.2%, 2.7%, and 3.9% for $L_{clad}=0.3$ nm, 1 nm, and 1.5 nm, respectively). Also, Table III shows that our calculated Coulomb shift varies from 107 meV to 96 meV and the exchange splitting from 1 meV to 0.8 meV when L_{clad} varies from 0.3 nm to 1.5 nm.

Including a finite barrier to represent the water solution and the Coulomb interaction between electron and hole, Weller and co-workers[3] used an effective mass model to calculate the $1S$-$1S$ transition energy $E_{1S\text{-}1S}^{weller}$ and Coulomb shifts E_{coul}^{weller} for the three CdS/HgS/CdS QDQW's. Their findings are also listed in Table III. The relative errors between their calculated $1S$-$1S$ transition energies and experimentally measured ones are 8%, 10%, and 11% for $L_{clad}=0.3$ nm, 1 nm, and 1.5 nm, respectively. The ETB theory clearly provides more accurate energy gaps than the effective-mass model. The predicted gaps of the ETB differ slightly from the measured gaps but are about 150 meV less than the prediction of the effective-mass model. Most of these differences are due to differences in the single-particle energies. The remaining part of the difference in energy gaps is due to the difference in Coulomb shifts. The Coulomb shifts predicted by effective-mass theory are 20 meV lower than the ETB results. It should also be noted that single-band effective mass theory[3,9] predicts the optically active $1S$-$1S$ transition to be the ground-state transition. Experiment[5] and tight-binding theory[11,12] show that the ground state is dark and must be the $1S$-$1P$ transition as we have calculated for the exciton ground state.

In the tight-binding model, the spin-orbit interaction is determined by the parameter $\lambda_i=\langle x_i,\uparrow|H_{so}|z_i,\downarrow\rangle$, where $i=a$ (anion) or c (cation) and H_{so} is the Hamiltonian of spin-orbit interaction.[18,19] In the bulk, it is known that the spin-orbit coupling lifts the degeneracy of the zone-center bulk band states and produces a fourfold degenerate state (the light and heavy hole bands) and a twofold degenerate state (the split-off band) at the zone center. For example, in bulk CdS, the zone-center splitting between the split-off band and the light and heavy hole bands is about 80 meV.[10] Bryant and Jaskólski[12] have shown that the spin-orbit splittings of single-particle states in the QDQW's are much smaller than the bulk zone-center ones. At large wave vector, the bulk CdS and HgS band structures show little effect of spin-orbit coupling. Spin-orbit effects and mixing are weak in QDQW's because the strongly confined trap states are made from bulk states with large wave vectors. Coulomb interaction does not strongly mix different levels, so our results should not change much when we include spin-orbit interaction. Detailed work about the effect of spin-orbit interaction on the fine structure of the excitonic spectrum is still in progress and will be reported in a future paper.

The ETB model we have considered for the QDQW has the following specific features: a spherical geometry, a particular well thickness and position inside the QDQW, no faceting of the surfaces or interfaces, a perfect fcc lattice, specific choices for uncertain material parameters (e.g., valence band offset, dielectric constant ϵ), and water barrier not included. However, the electronic structure obtained for the QDQW is determined mainly by the trapping and state symmetry and does not appear to depend significantly on the precise choices made specifically for QDQW geometry and

TABLE III. The Coulomb shift E_{coul}, exchange splitting E_{exch}, optical excitonic gap E_g^{opt}, and $1S$-$1S$ transition energy $E_{1S\text{-}1S}$ calculated for (4.7, 0.3, $L_{clad}=0.3$, 1, 1.5) CdS/HgS/CdS QDQW's. E_g^{exp} is the band gap measured by Weller and co-workers.[3] E_{coul}^{weller} and $E_{1S\text{-}1S}^{weller}$ are the Coulomb shift and $1S$-$1S$ transition energy, respectively, calculated with the effective-mass approximation.

L_{clad} (nm)	E_{coul} (meV)	E_{exch} (meV)	$E_{1S\text{-}1S}$ (eV)	E_g^{opt} (eV)	E_g^{exp} (eV)	$E_{1S\text{-}1S}^{weller}$ (eV)	E_{coul}^{weller} (meV)
0.3	107.00	1.07	2.10566	2.06719	2.10	2.27	84
1.0	98.33	0.88	2.01329	2.00183	1.96	2.16	76
1.5	96.66	0.85	2.01595	1.98951	1.94	2.15	75

material parameters. Bryant and Jaskólski[12] have tested this by studying single-particle states in QDQW's with different shapes and different well geometries and they have determined the dependence of the results on valence band offsets and spin-orbit coupling. For example, they have found that similar electron (hole) states exist for spherical, tetrahedral, and cutoff tetrahedral QDWS's provided that a similar number of cations (anions) occupy a particular region for each shape; the splitting between electron (hole) levels has a weak dependence on well thickness, well position, valence band offset, or as already mentioned, spin-orbit effects. The main effect of any of these uncertainties would be on the absolute energy position of the ground-state transition. The position of other transitions, relative to the ground-state transition, are insensitive to the uncertainties. Our good agreement with experiment shows that we also describe the lowest transition well with our model. The computational tests of Bryant and Jaskólski[12] are not exhaustive. Other possibilities (e.g., faceting at surfaces or interfaces, dependence on other tight-binding parameters, the dielectric screening, or on the effect of the water barrier) could be considered. However, further experimental characterization of QDQW geometry and material parameters and reduced experimental uncertainty are needed to provide tighter constraints for more complete sensitivity tests.

In summary, we have studied electron-hole correlations in QDQW's by incorporating Coulomb and exchange interactions into an empirical tight-binding model. Our calculated optical excitonic gaps are in good agreement with the experiment. Our ETB theory can provide a good description for QDQW nanocrystals.

S.L. acknowledges support of the DOE-BES-MS (DE-FG02-99ER45795) as well as the hospitality of the UIUC NCSA during 2001–2002.

*Corresponding author: FAX: (301) 990-1350. Email address: garnett.bryant@nist.gov

[1] P. Harrison, *Quantum Wells, Quantum Wires and Quantum Dots* (Wiley, New York, 2000).
[2] K. Barnham and D. Vvedensky, *Low-dimensional Semiconductor Structures: Fundamentals and Device Applications* (Cambridge University Press, New York, 2001).
[3] D. Schooss, A. Mews, A. Eychmüller, and H. Weller, Phys. Rev. B **49**, 17 072 (1994).
[4] A. Mews, A. Eychmüller, M. Giersig, D. Schooss, and H. Weller, J. Phys. Chem. **98**, 934 (1994).
[5] A. Mews, A.V. Kadavanich, U. Banin, and A.P. Alivisatos, Phys. Rev. B **53**, R13 242 (1996).
[6] S.V. Kershaw, M. Burt, M. Harrison, A. Rogach, H. Weller, and A. Eychmüller, Appl. Phys. Lett. **75**, 1694 (1999).
[7] R.B. Little, M.A. El-Sayed, G.W. Bryant, and S. Burke, J. Chem. Phys. **114**, 1813 (2001).
[8] J.W. Haus, H.S. Zhou, I. Honma, and H. Komiyama, Phys. Rev. B **47**, 1359 (1993).
[9] G.W. Bryant, Phys. Rev. B **52**, R16 997 (1995).
[10] W. Jaskólski and G.W. Bryant, Phys. Rev. B **57**, R4237 (1998).
[11] G.W. Bryant and W. Jaskólski, Physica E **11**, 72 (2001).
[12] G.W. Bryant and W. Jaskólski (unpublished).
[13] P.E. Lippens and M. Lannoo, Phys. Rev. B **39**, 10 935 (1989).
[14] K. Leung and K.B. Whaley, Phys. Rev. B **56**, 7455 (1997).
[15] K. Leung, S. Pokrant, and K.B. Whaley, Phys. Rev. B **57**, 12 291 (1998).
[16] S. Lee, L. Jönsson, J.W. Wilkins, G.W. Bryant, and G. Klimeck, Phys. Rev. B **63**, 195318 (2001).
[17] P. Vogl, H.P. Hjalmarson, and J.D. Dow, J. Phys. Chem. Solids **44**, 365 (1983).
[18] D.J. Chadi, Phys. Rev. B **16**, 790 (1977).
[19] K.C. Hass, H. Ehrenreich, and B. Velický, Phys. Rev. B **27**, 1088 (1983).
[20] L. Katsikas, A. Eychmüller, M. Giersig, and H. Weller, Chem. Phys. Lett. **172**, 201 (1990).